Effect of hydrogen bonding and complexation with metal ions on the fluorescence of luotonin A

Zsombor Miskolczy, László Biczók*

Institute of Molecular Pharmacology, Research Centre for Natural Sciences, Hungarian Academy of Sciences, P.O. Box 17, 1525 Budapest, Hungary

* Corresponding author. Fax: +36-1-438-1143; E-mail: biczok.laszlo@ttk.mta.hu

Abstract

Fluorescence characteristics of a biologically active natural alkaloid, luotonin A (LuA) was studied by steady-state and time-resolved spectroscopic methods. The rate constant of the radiationless deactivation from the singlet-excited state diminished by more than one order of magnitude when the solvent polarity was changed from toluene to water. Dual emission was found in polyfluorinated alcohols of large hydrogen bond donating power due to photoinitiated proton displacement along the hydrogen bond. In CH_2Cl_2, LuA produced both 1:1 and 1:2 hydrogen-bonded complexes with hexafluoro-2-propanol (HFIP) in the ground state. Photoexcitation of the 1:2 complex led to protonated LuA, whose fluorescence appeared at long wavelength. LuA served as a bidentate ligand forming 1:1 complexes with metal ions in acetonitrile. The stability of the complexes diminished in the series of Cd^{2+} > Zn^{2+} > Ag^{+}, and upon competitive binding of water to the metal cations. The effect of chelate formation on the fluorescent properties was revealed.

Key words: photoinduced protonation, dual fluorescence, chelate, excited-state deactivation, fluorescence lifetime, alkaloid

1. Introduction

Compounds composed of at least two nitrogen-heterocyclic rings have received considerable attention due to their versatile photophysical properties.[1-6] Light absorption of these species altered the charge density on the heteroatoms inducing considerable change in the acid-base strength. Consequently, photoinduced proton transfer or excited-state tautomerization could occur.[7-10] The effect of hydrogen bonding on the competition among the various deactivation pathways of excited azacarbazole alkaloids[11-16] _ENREF_11_ENREF_11 was revealed. The interaction with hydrogen bond acceptors and donors also led to substantial variation in the fluorescence characteristics of a pyridocarbazole alkaloid, ellipticine.[17-19] It was demonstrated that its dual fluorescence in methanol arose from excited state intermolecular proton transfer from the solvent to the nitrogen of the six-membered heterocyclic ring of the fluorophore.[19,20]

In the present work, we focused on the fluorescent behavior of luotonin A (LuA). This is a natural pyrroloquinazolinoquinoline alkaloid (Scheme1) isolated from the Chinese plant Peganum nigellastrum, which has been used for the treatment of rheumatism, abscess, and inflammation.[21,22] LuA also has antitumor activity,[23,24] and inhibits human DNA topoisomerase I enzyme.[25] Its _ENREF_1molecular structure resembles that of camptothecin derivatives employed in cancer chemotherapy.[26] Several routes have been developed for the synthesis of LuA and its analogues.[27-29] These compounds bind to the minor grove of the double-stranded DNA with equilibrium constants 220-1300 M^{-1} leading to fluorescence quenching.[30] LuA derivatives can be quantified by HPLC separation, and fluorimetric detection in human serum.[31]

Despite the biomedical importance of luotonin A, only very few information is available on its photophysical properties. The solvent, substituent and pH dependence of the fluorescence characteristics have been explored,[32] but time-resolved fluorescence measurements have not been performed. In the present paper, we reveal how the solvent

polarity and strong hydrogen bonding affect the kinetics of excited-state deactivation, and demonstrate that LuA can serve as a chelating agent for metal ions.

2. Experimental

Luotonin A (LuA) (Sigma), polyfluorinated alcohols (Aldrich) and metal salts (Aldrich) were used without further purification. Fluorescence quantum yields (Φ_f) were determined relative to that of quinine sulfate in 0.5 M H_2SO_4 solution, for which a reference yield of $\Phi_f = 0.546$ was taken.[33] The UV-visible absorption spectra were recorded on a Unicam UV 500 spectrophotometer. Corrected fluorescence spectra were obtained on a Jobin-Yvon Fluoromax-P spectrofluorometer. Fluorescence decays were measured with a time-correlated single-photon counting technique on a previously described apparatus.[34] Data were analyzed by a non-linear least-squares deconvolution method with Picoquant FluoFit software. All measurements were performed in air-saturated solutions at 297±2 K. The number of linearly independent absorbing or emitting species was determined by matrix rank analysis employing the program MRA 3.11 developed by Peintler et al.[35] The program can be downloaded from http://www.staff.u-szeged.hu/~peintler/enindex.htm. The concentration of LuA was measured spectrophotometrically using the molar absorption coefficient of $\varepsilon = 16860\ M^{-1}\ cm^{-1}$ at 358 nm in acetonitrile. This value agrees well with $\log \varepsilon / M^{-1}\ cm^{-1} = 4.21$ found in methanol.[21]

3. Results and discussion

Solvent effect on photophysical parameters

The quantum yield (Φ_f) and lifetime (τ_f) of the fluorescence of LuA exhibited marked solvent dependence (Table 1). As a measure of solvent polarity, E_T^N parameter[36] was used. One order of magnitudes increase in Φ_f was observed when the solvent was changed from toluene to

water reaching a value of 0.46. A concomitant significant lengthening of τ_f was also obtained. The Φ_f data found in this work in ethanol and acetonitrile are in accordance with the reported values,[32] whereas our result in water is somewhat larger than $\Phi_f = 0.314$, the value previously found[32] at pH 5.5. The rate constants of fluorescence emission (k_f) and radiationless deactivation (k_{nr}) from the singlet excited state were calculated using $k_f = \Phi_f/\tau_f$ and $k_{nr} = (1-\Phi_f)/\tau_f$ relationships. The former quantity slightly diminished with the growth of the solvent polarity, while k_{nr} significantly decreased indicating that the radiationless deactivation was more sensitive to the polarity and hydrogen bond donor ability of the microenvironment. The solvent dependence of k_{nr} of LuA proved to be much larger than that of the structurally related alkaloid, camptothecin.[37] For the latter compound, k_{nr} diminished only by a factor about 2 from cyclohexane ($k_{nr} = 1.91 \times 10^8$ s^{-1}) to water ($k_{nr} = 0.90 \times 10^8$ s^{-1}). The quicker radiationless energy dissipation in nonpolar medium was attributed to the more efficient vibronic interaction between the close-lying $S_1(\pi\pi^*)$ and $S_2(n\pi^*)$ excited states.[37] Lim demonstrated for many nitrogen heterocyclic and aromatic carbonyl compounds that vibronic coupling between nearby $\pi\pi^*$and $n\pi^*$ singlet states induced a very efficient internal conversion.[38] This phenomenon is widely known as ”proximity effect”. Both hydrogen bonding and solvent polarity growth displace the $\pi\pi^*$ states toward lower energy, whereas the $n\pi^*$ states are moved to higher energy. Consequently, the $S_1(\pi\pi^*)$–$S_2(n\pi^*)$ energy gap in LuA increases with polarity leading thereby to reduced coupling between the two excited states, which decelerates internal conversion. The more rapid radiationless depopulation of the singlet-excited LuA compared to camptothecin suggests that the energy difference between $S_1(\pi\pi^*)$ and $S_2(n\pi^*)$ states is smaller in the former alkaloid. The much smaller k_{nr} of LuA in water than in ethanol reflects the more substantial effect of the stronger dipole-dipole and hydrogen bonding interactions on the $S_1(\pi\pi^*)$–$S_2(n\pi^*)$ energy gap in aqueous medium.

LuA exhibited entirely different behavior in solvents of large hydrogen bond donating ability. As seen in Figure 1, dual emission was observed in 2,2,2-trifluoroethanol (TFE) and 1,1,1,3,3,3-hexafluoro-2-propanol (HFIP). The excitation spectra were identical irrespective of the detection wavelength, and corresponded to the absorption spectrum. The long-wavelength band resembled that reported for protonated luotonin A ($LuAH^+$) in acidic aqueous solution.[32] Thus, we conclude that hydrogen bonding promoted the photoinduced protonation of LuA in TFE and HFIP. Since this process was more efficient in a solvent of larger hydrogen bond donating power, more intense long-wavelength emission was detected in HFIP. Abraham's hydrogen bond acidity parameters ($\Sigma\alpha_2^H$) are 0.35, 0.57 and 0.77 for water, TFE and HFIP, respectively.[39,40] The growth of $\Sigma\alpha_2^H$ in this series indicates the strengthening of the hydrogen bond with the solute and the rising ability of the solvents to donate proton along the hydrogen bond. The absorption spectra of LuA in TFE and HFIP barely differ from those in other solvents indicating that LuA is not protonated in the ground state.

Effect of hydrogen bonding in CH_2Cl_2

To gain insight into the details of the photophysical processes initiated by hydrogen bonding, the effect of HFIP was examined in CH_2Cl_2. The gradual addition of HFIP brought about a bathochromic shift in the absorption spectrum, and isosbestic points developed at 331, 341, 359 and 364 nm in the 0-0.06 M HFIP range (Figure 2A). At larger HFIP concentrations, further spectral changes were observed and the isosbestic points blurred suggesting that not only 1:1 binding occurred. The protonation of LuA in the ground state was excluded, because the spectrum did not extend above 390 nm, where $LuAH^+$ absorbs light.[32]

The equilibrium constants of 1:1 (K_1) and 1:2 (K_2) complexes were calculated by global analysis of the experimental results in the 330-390 nm range. Since HFIP was added in a large excess compared to LuA, the absorbance change was described by the function:

$$A_\lambda = A_\lambda^0 \left(\frac{1 + \varepsilon_1^\lambda / \varepsilon_0^\lambda K_1[HFIP] + \varepsilon_2^\lambda / \varepsilon_1^\lambda K_2 K_1 [HFIP]^2}{1 + K_1[HFIP] + K_2 K_1 [HFIP]^2} \right) \quad (1)$$

where ε_0^λ, ε_1^λ and ε_2^λ are the molar absorption coefficients at a particular wavelength (λ) for free LuA, 1:1 and 1:2 complexes, respectively. A^0_λ and A_λ denote the absorbances in the absence and the presence of HFIP. The nonlinear least squares fit provides $K_1 = 73\ M^{-1}$ and $K_2 = 3\ M^{-1}$ for the binding constant of the consecutive two steps of complexation. The lines in Figure 2B present the calculated data.

Addition of 0-0.06 M HFIP to LuA in CH_2Cl_2 caused a considerable fluorescence enhancement, and about 14 nm red-shift of the fluorescence maximum due to 1:1 hydrogen bonding. Further increase of HFIP concentration led to quenching of this band accompanied by the emergence of a new emission centered at 515 nm with an isoemissive point at 473 nm (Figure 3). The long-wavelength fluorescence band was assigned to protonated luotonin A ($LuAH^+$) because it matched the spectrum of $LuAH^+$ in 0.04 M trifluoroacetic acid CH_2Cl_2 solution. Similar spectra have been reported for protonated LuA derivatives in water.[32]

To gain insight into the kinetics of photoinitiated processes, time-resolved measurements were performed. The deduced reaction mechanism is presented in Scheme 2. Three fluorescence components were detected at 400 nm, whose 0.37, 1.4 and 0.70 ns lifetimes were independent of HFIP concentration implying that no dynamic quenching occurred. The shortest-lived component ($\tau_1 = 0.37$ ns) was attributed to the uncomplexed LuA because the same decay time was obtained in neat CH_2Cl_2. The gradual increase of HFIP concentration diminished the amplitude of LuA emission (a_1), and strengthened the fluorescence of $\tau_2 = 1.4$ ns. Since these changes occurred parallel to the alteration of the absorption and fluorescence spectra in the 0-0.06 M HFIP concentration range (vide supra), τ_2 was assigned to the fluorescence of 1:1 hydrogen-bond complex. The amplitude of this emission (a_2) reached a maximum in the presence of about 0.06 M HFIP, and then declined

due to the growth of the intensity of the emission of τ_3 = 0.70 ns. The latter component originated from 1:2 complex. Figure 4 presents the variation of the relative amplitudes ($a_n/\sum|a_n|$) with HFIP concentration.

The long-wavelength emission was examined at 550 nm, where the uncomplexed LuA weakly fluoresces. Since the tail of the short-wavelength band extends beyond 550 nm, the fluorescence of 1:1 complex with 1.4 ns lifetime could be detected. In addition, $LuAH^+$ emission was detected with 0.7 ns rise time and 4.6 ns decay time. The build-up of $LuAH^+$ fluorescence corresponded to the lifetime of the singlet-excited 1:2 complex indicating that the transformation of the 1:2 complex to $LuAH^+$ occurred predominantly in the singlet-excited state. The amplitudes of the rise and decay of $LuAH^+$ fluorescence showed no systematic differences apart from their opposite sign (Figure 4B) suggesting that $LuAH^+$ was produced by proton transfer within the excited 1:2 complex. The very small absorption above 400 nm also implied that insignificant amount of $LuAH^+$ was formed in the ground state. The opposite change of the amplitudes of the decay components possessing τ_2 = 1.4 ns and τ_3 = 0.70 ns originated from the conversion of 1:1 complex to 1:2 complex in the ground state upon increase of HFIP concentration. The photoexcitation of the latter species led to $LuAH^+$.

When the much weaker hydrogen bond donor TFE was used as additive in CH_2Cl_2, the fluorescence maximum of LuA shifted from 400 to 410 nm in 0.4 M TFE solution, and a 2.23-fold increase in Φ_f was observed. However, no long-wavelength band emerged, and the lifetime was 1.0 ns irrespective of the detection wavelength. These implied that no photoinduced proton transfer took place within LuA-TFE hydrogen bond complex. The fluorescence quantum yield enhancement arose from the decelerated radiationless deactivation of the excited hydrogen bond complex. The small alteration of the absorption spectrum indicated hydrogen bonding in the ground state.

Complexation with Cd^{2+} and Zn^{2+} ions

As shown in Figure 5, addition of $Cd(ClO_4)_2$ to LuA in acetonitrile resulted in the emergence of a new red-shifted band in both the absorption and fluorescence spectra. The isosbestic points at 251, 276.5 and 346 nm, as well as the isoemissive point at 416 nm suggested that 1:1 complexation occurred under our experimental condition. LuA acted as a bidentate ligand binding with its nitrogens located at the 5- and 6-positions to the metal ion. The equilibrium constant (K) was determined from the absorbance (A) change with cation concentration using the following relationship:[41]

$$A = A_0 + \frac{A_\infty - A_0}{2}\left\{1 + \frac{[\text{cation}]_0}{[\text{LuA}]_0} + \frac{1}{K[\text{LuA}]_0} - \left[\left(1 + \frac{[\text{cation}]_0}{[\text{LuA}]_0} + \frac{1}{K[\text{LuA}]_0}\right)^2 - 4\frac{[\text{cation}]_0}{[\text{LuA}]_0}\right]^{\frac{1}{2}}\right\} \quad (2)$$

where $[LuA]_0$ represents the initial alkaloid concentration, whereas A_∞ and A_0 denote the absorbance of the fully complexed and free LuA, respectively. The global nonlinear least-squares fit of the experimental data gave K = 8300 M^{-1} for 1:1 association of Cd^{2+} with LuA. Similar analysis of the fluorescence titration data provided K = 7700 M^{-1} in fair agreement with the results derived from the absorption spectra. The insets to Figure 5 demonstrate that the calculated functions match the experimental data.

Addition of $Zn(NO_3)_2$ caused a similar spectral change, but the driving force of Zn^{2+} complexation was significantly smaller than that of Cd^{2+}. The equilibrium constants derived from spectrophotometric and fluorescence spectroscopic titrations are summarized in Table 2. The larger stability of the Cd^{2+} complex may originate partly from the better match of the ion size and the structural features of LuA compared to the smaller Zn^{2+}. The weaker solvent-solute interaction with the bulkier Cd^{2+} also contributed to its larger binding affinity. The quantum yields and lifetimes of fluorescence were 0.13 and 0.94 ns for Cd^{2+}-LuA, whereas 0.25 and 2.4 ns were found for Zn^{2+}-LuA. The difference in these photophysical parameters

may stem primarily from the more substantial heavy atom effect of Cd^{2+}, which promoted more rapid radiationless deactivation from the singlet-excited state.

To confirm the number of light absorbing and fluorescent species, matrix rank analysis of the spectra was carried out. The residual absorbance and fluorescence intensity curves exhibited random distribution in the case of two absorbing or fluorescent species implying that LuA produced only 1:1 complex with Cd^{2+} and Zn^{2+} under the conditions of our studies.

Solvent effect on the stability and fluorescence of metal complexes

To reveal how the interaction with solvent influences the stability and fluorescent characteristics of LuA complexes, experiments were performed in acetonitrile-water mixtures. Figure 6A displays the variation of the fluorescence spectrum of Zn^{2+}-LuA with the water content of the medium. The diminution of the intensity of the complex emission was accompanied by the rise of the blue-shifted free LuA fluorescence upon progressive addition of water. This suggested that the metal complex became less stable when the water content of the solution was increased. The growth of the fluorescence intensity after the complete disappearance of Zn^{2+}-LuA was in accordance with the fluorescence quantum yield enhancement of LuA in polar hydrogen bonding medium (vide supra).

The gradual dissociation of Zn^{2+}-LuA with increasing water concentration was also followed by time-resolved measurements. The single-exponential fluorescence decay in Zn^{2+}-LuA solution turned to dual-exponential upon addition of water. The lifetime of the excited Zn^{2+}-LuA complex remained constant (2.4 ns), and the diminution of the amplitude of this fluorescence component with growing water concentration was accompanied by the emergence of a shorter-lived emission (Figure 6B). This fluorescence component was attributed to free LuA because it had practically identical decay kinetics to that of LuA in the corresponding acetonitrile-water mixture. The fluorescence lifetime was significantly lengthened by water for uncomplexed LuA (Figure 6C) due to the deceleration of the rate of

radiationless deactivation from the singlet-excited state, but remained unaltered in the case of Zn^{2+}-LuA. The relative amplitude of Zn^{2+}-LuA fluorescence gradually lessened and completely vanished in the presence of around 7 M water (Figure 6B) because coordination of water to Zn^{2+} and hydrogen bonding with the heterocyclic nitrogens located at 5- and 6-positions of LuA efficiently competed with Zn^{2+}-LuA formation.

Addition of water affected the fluorescent properties of Cd^{2+}-LuA analogously to that found for Zn^{2+}-LuA, but the changes occurred at larger water concentration. Figure 7 demonstrates that more water is needed to eliminate the binding of Cd^{2+} to LuA. The difference in the affinity to water is due to the 47.8 kJ mol^{-1} less negative free energy of hydration[42,43] for Cd^{2+} compared to that of Zn^{2+}. The equilibrium constant of Cd^{2+} complex formation (K) is about 30-fold smaller in the presence of 3.5 M water than in neat acetonitrile, whereas 22-fold diminution in K takes place in ethanol compared to the value in acetonitrile (Table 2). The difference in K values results primarily from the lessening of the Gibbs free energy of Cd^{2+} solvation in the series of acetonitrile, ethanol and water.[44]

Ag^+ binding

Complexation with Ag^+ brought about similar alteration in the absorption spectrum of LuA to that shown in Figure 5A, but the binding affinity was significantly lower than in the case of Cd^{2+} (Table 2). Ag^+ quenched the fluorescence of LuA without altering the shape of the fluorescence spectrum (Figure 8). The lack of a new band implied that Ag^+-LuA was non-fluorescent. Excited state charge transfer within the complex probably induced efficient radiationless energy dissipation. The reciprocal emission intensity exhibited an excellent linear correlation as a function of Ag^+ concentration. The invariant fluorescence lifetime suggested that no dynamic quenching occurred. Thus, the slope of the Stern-Volmer plot (510 M^{-1}) corresponded to the equilibrium constant of Ag^+ association with LuA in the ground

state. The results of the nonlinear least-squares analysis of the absorption and fluorescence data are given in Table 2. In contrast to the considerable water effect on the binding affinity of Cd^{2+} and Zn^{2+}, the stability of Ag^{+}-LuA complex decreased only a small extent upon addition of 3.5 M water. The different behavior was ascribed to the strong preferential solvation of the monovalent ions by acetonitrile, whereas the divalent ions were preferentially solvated by the water component in water-acetonitrile mixtures.[45] It was demonstrated that the standard molar free energies of the transfer of ions from acetonitrile to water are 23.2, –42.2 and –68.7 $kJmol^{-1}$ for Ag^{+}, Cd^{2+} and Zn^{2+}, respectively.[44] The substantial rise of exothermicity explains the increase of water sensitivity of the LuA complexes in the series of these cations. The strength of the coordination of water to metal cation is the dominant factor controlling the driving force of metal complex formation. The hydrogen bonding of LuA to water has less significant influence.

4. Conclusions

The fluorescence properties of LuA were sensitive to the bulk polarity of the microenvironment and specific hydrogen bonding interactions alike. The increase of the former factor decelerated the radiationless deactivation from the singlet-excited state, whereas the latter effect facilitated photoinduced proton transfer in solvents of strong hydrogen bond donor character. Binding of at least two HFIP was needed to bring about proton transfer to singlet-excited LuA. The formation of 1:1 complex with metal ions in acetonitrile significantly altered the fluorescence of LuA. Ag^{+}-LuA proved to be nonemitting. The quantum yield and lifetime of the fluorescence were larger for Zn^{2+}-LuA than the corresponding values of Cd^{2+}-LuA, but the binding affinity exhibited reverse trend. Coordination of water to the metal ions influenced the stability of chelates much more significantly than the hydrogen bonding with LuA. The results may be utilized in the design of fluorescent probes for selective detection of Ag^{+}, Zn^{2+} or Cd^{2+} cations.

Acknowledgement

The authors very much appreciate the support of this work by the Hungarian Scientific Research Fund (OTKA, Grant K104201).

References

1 J. Waluk, Hydrogen-bonding-induced phenomena in bifunctional heteroazaaromatics, *Acc. Chem. Res.*, 2003, **36**, 832-838.

2 J. Dobkowski, J. Herbich, V. Galievsky, R. P. Thummel, F. Y. Wu and J. Waluk, Diversity of excited state deactivation paths in heteroazaaromatics with multiple intermolecular hydrogen bonds, *Ber. Bunsen-Ges. Phys. Chem.*, 1998, **102**, 469-475.

3 V. Vetokhina, K. Dobek, M. Kijak, I. I. Kamińska, K. Muller, W. R. Thiel, J. Waluk and J. Herbich, Three Modes of Proton Transfer in One Chromophore: Photoinduced Tautomerization in 2-(1H-Pyrazol-5-yl)Pyridines, Their Dimers and Alcohol Complexes, *ChemPhysChem*, 2012, **13**, 3661-3671.

4 C. C. Cheng, C. P. Chang, W. S. Yu, F. T. Hung, Y. I. Liu, G. R. Wu and P. T. Chou, Comprehensive studies on dual excitation behavior of double proton versus charge transfer in 4-(N-substituted amino)-1H-pyrrolo 2,3-b pyridines, *J. Phys. Chem. A*, 2003, **107**, 1459-1471.

5 P. Nikolov and H. Görner, Excimer fluorescence from acridine and diaza-heterocyclic hydrocarbons in non-polar media at low temperatures, *J. Photochem. Photobiol. A: Chem.*, 1996, **101**, 137-144.

6 Z. Miskolczy, M. Megyesi, L. Biczók and H. Görner, Effect of electrolytes, nucleotides and DNA on the fluorescence of flavopereirine natural alkaloid, *Photochem. Photobiol. Sci.*, 2011, **10**, 592-600.

7 J. C. Penedo, J. L. P. Lustres, I. G. Lema, M. C. R. Rodríguez, M. Mosquera and F. Rodríguez-Prieto, Solvent-Dependent Ground- and Excited-State Tautomerism in 2-(6‘-Hydroxy-2‘-pyridyl)benzimidazole, *J. Phys. Chem. A*, 2004, **108**, 6117-6126.

8 A. Maliakal, G. Lem, N. J. Turro, R. Ravichandran, J. C. Suhadolnik, A. D. DeBellis, M. G. Wood and J. Lau, Twisted intramolecular charge transfer states in 2-arylbenzotriazoles: Fluorescence deactivation via intramolecular electron transfer rather than proton transfer, *J. Phys. Chem. A*, 2002, **106**, 7680-7689.

9 S. Takeuchi and T. Tahara, The answer to concerted versus step-wise controversy for the double proton transfer mechanism of 7-azaindole dimer in solution, *Proc. Natl. Acad. Sci. USA*, 2007, **104**, 5285-5290.

10 P. Toele, H. Zhang and M. Glasbeek, Femtosecond fluorescence anisotropy studies of excited-state intramolecular double-proton transfer in 2,2 '-bipyridyl -3,3-diol in solution, *J. Phys. Chem. A*, 2002, **106**, 3651-3658.

11 D. Reyman, M. J. Tapia, C. Carcedo and M. H. Viñas, Photophysical properties of methyl β-carboline-3-carboxylate mediated by hydrogen-bonded complexes - A comparative study in different solvents, *Biophys. Chem.*, 2003, **104**, 683-696.

12 P. T. Chou, Y. I. Liu, G. R. Wu, M. Y. Shiao, W. S. Yu, C. C. Cheng and C. P. Chang, Proton-transfer tautomerism of β-carbolines mediated by hydrogen-bonded complexes, *J. Phys. Chem. B*, 2001, **105**, 10674-10683.

13 D. Reyman, C. Diaz-Oliva, F. Hallwass and S. M. Goncalves de Barros, New insights into the photo-tautomerisation process in [small beta]-carboline derivatives revealed by NMR spectroscopy, *RSC Advances*, 2011, **1**, 857-865.

14 A. Sánchez-Coronilla, M. Balón, M. A. Muñoz, J. Hidalgo and C. Carmona, Ground state isomerism in betacarboline hydrogen bond complexes: The charge transfer nature of its large Stokes shifted emission, *Chem. Phys.*, 2008, **351**, 27-32.

15 C. Carmona, M. Balón, A. S. Coronilla and M. A. Muñoz, New Insights on the Excited-State Proton-Transfer Reactions of Betacarbolines: Cationic Exciplex Formation, *J. Phys. Chem. A*, 2004, **108**, 1910-1918.

16 C. Carmona, M. Galan, G. Angulo, M. A. Munoz, P. Guardado and M. Balon, Ground and singlet excited state hydrogen bonding interactions of betacarbolines, *Phys. Chem. Chem. Phys.*, 2000, **2**, 5076-5083.

17 Z. Miskolczy and L. Biczók, Fluorescent properties of hydrogen-bonded ellipticine: A special effect of fluoride anion, *J. Photochem. Photobiol. A: Chem.*, 2006, **182**, 82-87.

18 S. Y. Fung, J. Duhamel and P. Chen, Solvent Effect on the Photophysical Properties of the Anticancer Agent Ellipticine, *J. Phys. Chem. A*, 2006, **110**, 11446-11454.

19 Z. Miskolczy, L. Biczók and I. Jablonkai, Effect of hydroxylic compounds on the photophysical properties of ellipticine and its 6-methyl derivative: The origin of dual fluorescence, *Chem. Phys. Lett.*, 2006, **427**, 76-81.

20 Z. Miskolczy, L. Biczók and I. Jablonkai, Comment on "Dual Fluorescence of Ellipticine: Excited State Proton Transfer from Solvent versus Solvent Mediated Intramolecular Proton Transfer", *J. Phys. Chem. A*, 2012, **116**, 899-900.

21 Z. Z. Ma, Y. Hano, T. Nomura and Y. J. Chen, Two new pyrroloquinazolinoquinoline alkaloids from Peganum nigellastrum, *Heterocycles*, 1997, **46**, 541-546.

22 J. L. Liang, H. C. Cha and Y. Jahng, Recent Advances in the Studies on Luotonins, *Molecules*, 2011, **16**, 4861-4883.

23 J. S. Yadav and B. V. S. Reddy, Microwave-assisted rapid synthesis of the cytotoxic alkaloid luotonin A, *Tetrahedron Lett.*, 2002, **43**, 1905-1907.

24 S. Dallavalle, L. Merlini, G. L. Beretta, S. Tinelli and F. Zunino, Synthesis and cytotoxic activity of substituted Luotonin A derivitives, *Bioorg. Med. Chem. Lett.*, 2004, **14**, 5757-5761.

25 A. Cagir, S. H. Jones, R. Gao, B. M. Eisenhauer and S. M. Hecht, Luotonin A. A naturally occurring human DNA topoisomerase I poison, *J. Am. Chem. Soc.*, 2003, **125**, 13628-13629.

26 Q. Y. Li, Y. G. Zu, R. Z. Shi and L. P. Yao, Review Camptothecin: Current Perspectives, *Curr. Med. Chem.*, 2006, **13**, 2021-2039.

27 H. B. Zhou, G. S. Liu and Z. J. Yao, Short and efficient total synthesis of luotonin a and 22-hydroxyacuminatine using a common cascade strategy, *J. Org. Chem.*, 2007, **72**, 6270-6272.

28 J. J. Mason and J. Bergman, Total synthesis of luotonin A and 14-substituted analogues, *Org. Biomol. Chem.*, 2007, **5**, 2486-2490.

29 M. C. Tseng, Y. W. Chu, H. P. Tsai, C. M. Lin, J. L. Hwang and Y. H. Chu, One-Pot Synthesis of Luotonin A and Its Analogues, *Org. Lett.*, 2011, **13**, 920-923.

30 P. Mussardo, E. Corda, V. Gonzalez-Ruiz, J. Rajesh, S. Girotti, M. A. Martin and A. I. Olives, Study of non-covalent interactions of luotonin A derivatives and the DNA minor groove as a first step in the study of their analytical potential as DNA probes, *Anal. Bioanal. Chem.*, 2011, **400**, 321-327.

31 V. Gonzalez-Ruiz, P. Mussardo, E. Corda, S. Girotti, A. I. Olives and M. A. Martin, Liquid chromatographic analysis of the anticancer alkaloid luotonin A and some new derivatives in human serum samples, *J. Sep. Sci.*, 2010, **33**, 2086-2093.

32 V. Gonzalez-Ruiz, Y. Gonzalez-Cuevas, S. Arunachalam, M. A. Martin, A. I. Olives, P. Ribelles, M. T. Ramos and J. C. Menendez, Fluorescence properties of the anti-tumour alkaloid luotonin A and new synthetic analogues: pH modulation as an approach to their fluorimetric quantitation in biological samples, *J. Luminesc.*, 2012, **132**, 2468-2475.

33 W. H. Melhuish, Quantum efficiencies of fluorescence of organic substances: Effect of solvent and concentration of the fluorescent solute, *J. Phys. Chem.*, 1961, **65**, 229-235.

34 K. Nagy, S. Göktürk and L. Biczók, Effect of microenvironment on the fluorescence of 2-hydroxy-substituted Nile Red dye: A new fluorescent probe for the study of micelles, *J. Phys. Chem. A*, 2003, **107**, 8784-8790.

35 G. Peintler, I. Nagypál, A. Jancsó, I. R. Epstein and K. Kustin, Extracting Experimental Information from Large Matrixes. 1. A New Algorithm for the Application of Matrix Rank Analysis, *J. Phys. Chem. A*, 1997, **101**, 8013-8020.

36 C. Reichardt, Solvatochromic dyes as solvent polarity indicators, *Chem. Rev.*, 1994, **94**, 2319-2358.

37 J. Dey and I. M. Warner, Spectroscopic and photophysical studies of the anticancer drug: Camptothecin, *J. Luminesc.*, 1997, **71**, 105-114.

38 E. C. Lim, Proximity effect in molecular photophysics: dynamical consequences of pseudo-Jahn-Teller interaction, *J. Phys. Chem.*, 1986, **90**, 6770-6777.

39 M. H. Abraham, P. L. Grellier, D. V. Prior, P. P. Duce, J. J. Morris and P. J. Taylor, Hydrogen bonding. Part 7. A scale of solute hydrogen-bond acidity based on log K values for complexation in tetrachloromethane, *Journal of the Chemical Society, Perkin Transactions 2*, 1989, **0**, 699-711.

40 M. H. Abraham, Scales of solute hydrogen-bonding: their construction and application to physicochemical and biochemical processes, *Chem. Soc. Rev.*, 1993, **22**, 73-83.

41 B. Valeur, *Molecular Fluorescence, Principles and Applications*, Wiley-VCH, Weinheim, 2002.

42 Y. Marcus, A simple empirical model describing the thermodynamics of hydration of ions of widely varying charges, sizes, and shapes, *Biophys. Chem.*, 1994, **51**, 111-127.

43 C. S. Babu and C. Lim, Empirical Force Fields for Biologically Active Divalent Metal Cations in Water, *J. Phys. Chem. A*, 2005, **110**, 691-699.

44 Y. Marcus, M. J. Kamlet and R. W. Taft, Linear solvation energy relationships: standard molar Gibbs free energies and enthalpies of transfer of ions from water into nonaqueous solvents, *J. Phys. Chem.*, 1988, **92**, 3613-3622.

45 Y. Marcus, Preferential solvation of silver(I), copper(I) and copper(II) ions in aqueous acetonitrile, *J. Chem. Soc., Dalton Trans.*, 1991, 2265-2268.

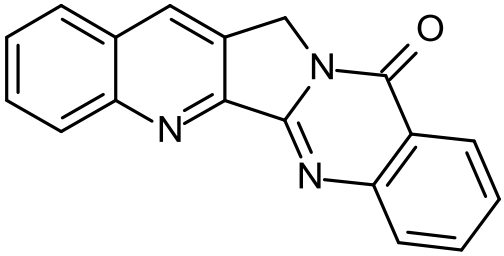

Scheme 1. The formula of luotonin A

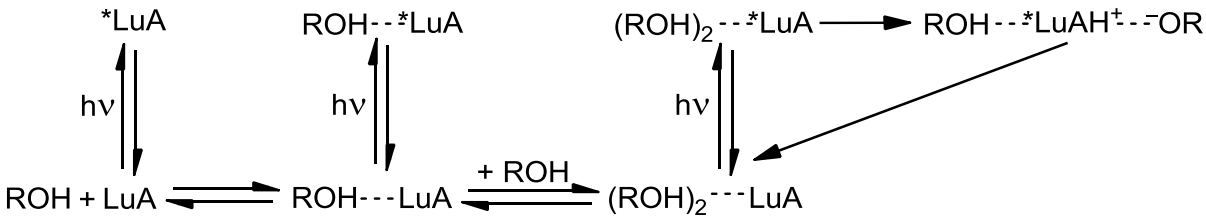

Scheme 2. Reaction steps in the presence of hexafluoro-2-propanol (ROH) in CH_2Cl_2

Table 1. Photophysical properties of luotonin A in solvents of different polarity

Solvent	E_T^N	Φ_f	τ_f / ns	k_f / 10^8 s^{-1}	k_{nr} / 10^8 s^{-1}
toluene	0.099[a]	0.046	0.15	3.1	64
CH_2Cl_2	0.309[a]	0.098	0.37	2.6	24
CH_3CN	0.460[a]	0.082	0.43	1.9	21
CH_3CH_2OH	0.654[a]	0.10	0.54	1.9	17
H_2O	1[a]	0.46	2.7	1.7	2.0

[a] Solvent polarity parameters[36]

Table 2. Equilibrium constants and fluorescence lifetimes of metal ion-LuA complexes in various solvents

Additive	Solvent	K / M^{-1} from absorption	K / M^{-1} from fluorescence	τ_f / ns
$Cd(ClO_4)_2$	CH_3CN	8300	7700	0.94
$Cd(ClO_4)_2$	CH_3CN + 3.5 M H_2O	250	260	1.1
$CdCl_2$	EtOH	350	380	1.1
$Zn(NO_3)_2$	CH_3CN	1100	1100	2.4
$Zn(NO_3)_2$	CH_3CN + 3.5 M H_2O	[a]	[a]	[a]
$AgNO_3$	CH_3CN	490	510	[b]
$AgNO_3$	CH_3CN + 3.5 M H_2O	430	460	[b]

[a] negligible binding affinity, [b] nonfluorescent complex

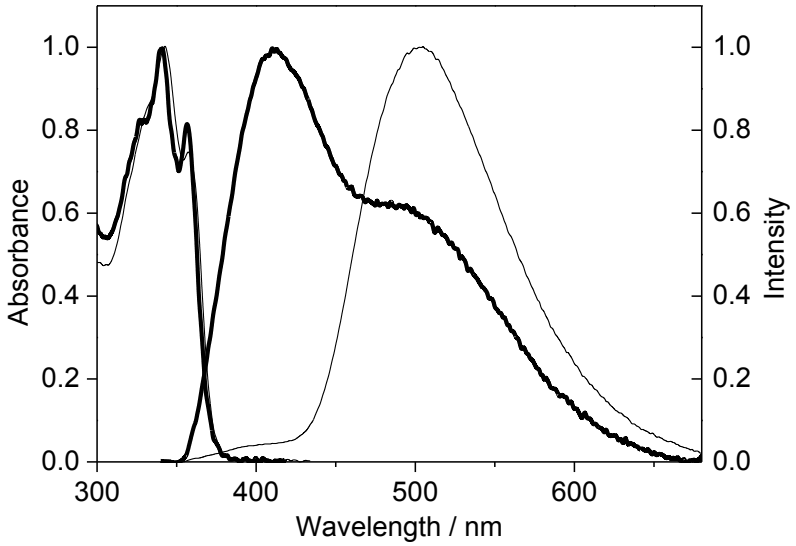

Figure 1. Absorption and fluorescence spectra of LuA in TFE (thick line) and HFIP (thin line).

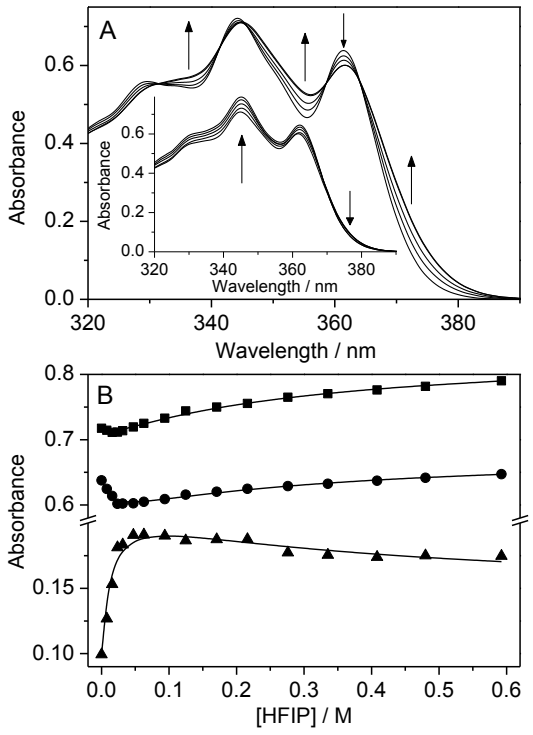

Figure 2. (A) Absorption spectrum of LuA in the presence of 0, 7.9, 16, 24 and 32 mM HFIP in in CH_2Cl_2. Inset: [HFIP] = 0.032, 0.094, 0.22, 0.41 and 0.59 M. (B) Absorbance change at 345 (■), 362 (●) and 373 nm (▲). The lines show the fitted function.

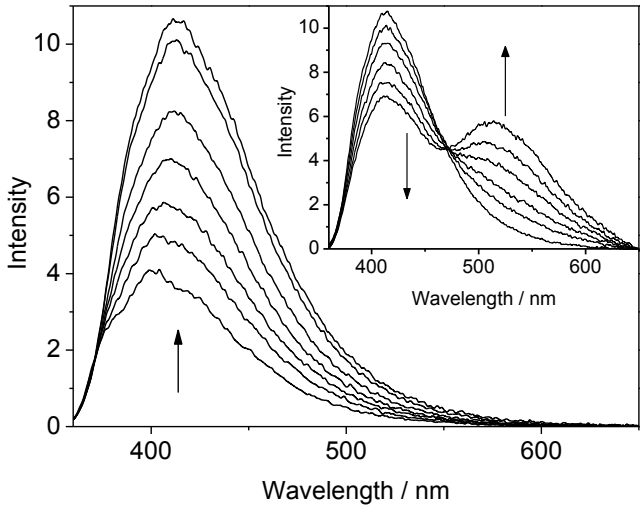

Figure 3. Fluorescence spectrum of LuA in the presence of 0, 2.4, 4,8, 9.5, 19, 42 and 65 mM HFIP in in CH_2Cl_2. Inset: [HFIP] = 0.10, 0.22, 0.30, 0.40, 0.49 and 0.58 M. Excitation wavelength (λ_{exc}) is 358 nm.

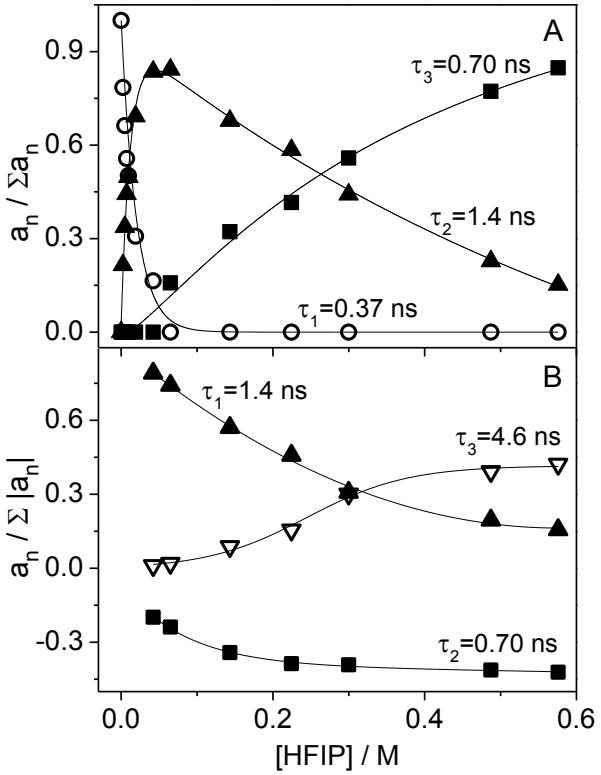

Figure 4. Variation of the relative amplitudes of the fluorescence decay components as a function of HFIP concentration in CH_2Cl_2. Detection at 400 nm (A) and 550 nm (B).

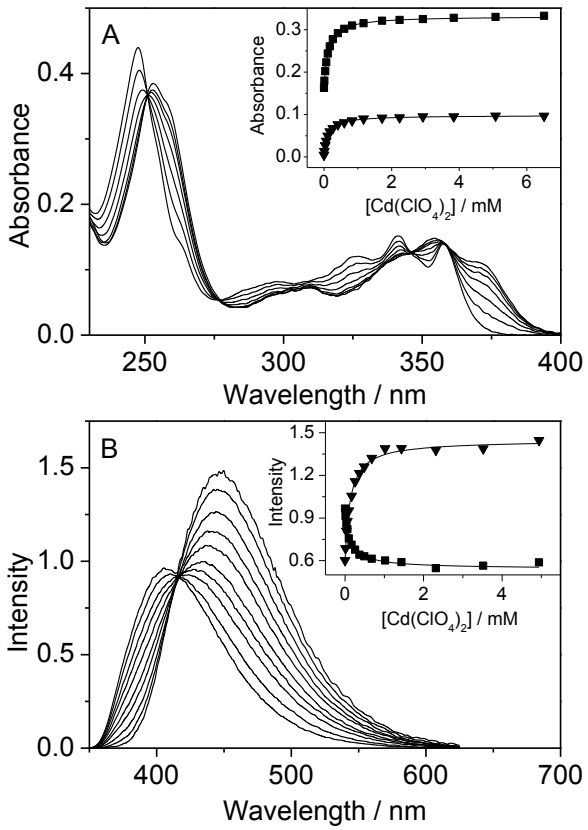

Figure 5. (A) Effect of 0, 0.037, 0.11, 0.26, 0.60, 1.2 and 6.5 mM $Cd(ClO_4)_2$ on the absorption spectrum of 8.35 μM LuA in CH_3CN. Inset displays the absorbances at 260 (■) and 375 nm (▼) and the lines are the result of nonlinear least-squares fit. (B) Alteration of the fluorescence spectrum of 7.3 μM LuA upon addition of 0, 0.012, 0.037, 0.061, 0.097, 0.17, 0.26, 0.49, 1.0 and 4.9 mM $Cd(ClO_4)_2$ in CH_3CN. Inset shows the fluorescence intensity at 405 (■) and 445 nm (▼) and the lines represent the best fit.

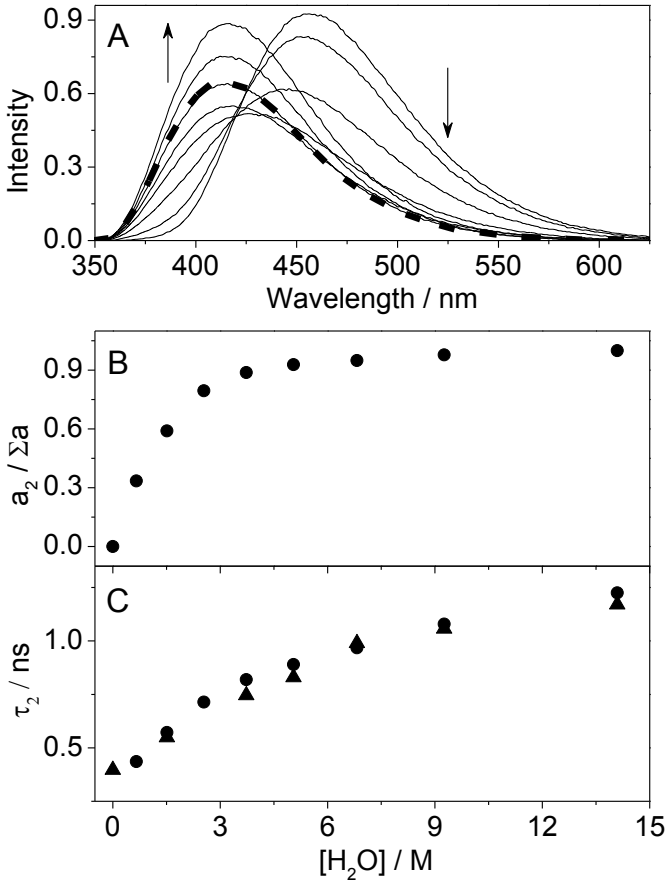

Figure 6. (A) Change of the fluorescence spectra of Zn^{2+}-LuA complex upon addition of 0, 0.55, 1.4, 2.4, 3.6, 6.8, 12 and 19 M water in CH_3CN. ([LuA] = 8.2 μM, [Zn^{2+}] = 0.02 M, λ_{exc}=346 nm) The thick dashed line presents the fluorescence spectrum of LuA in CH_3CN + 6.8 M water mixture in the absence of Zn^{2+}. Relative amplitudes (B) and the fluorescence lifetime (C) of uncomplexed LuA as a function of water concentration in acetonitrile containing 8.2 μM LuA + 0.01 M Zn^{2+}. The triangles display the lifetimes in the absence of Zn^{2+}.

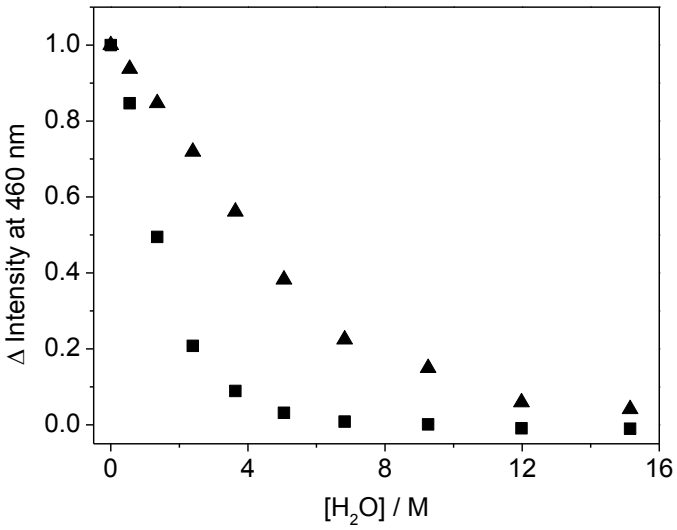

Figure 7. Difference of the fluorescence intensities at 460 nm in the presence and absence of 0.02 M Cd^{2+} (▲) or Zn^{2+} (■) as a function of water concentration in CH_3CN. ([LuA] = 8.2 μM, λ_{exc}=346 nm)

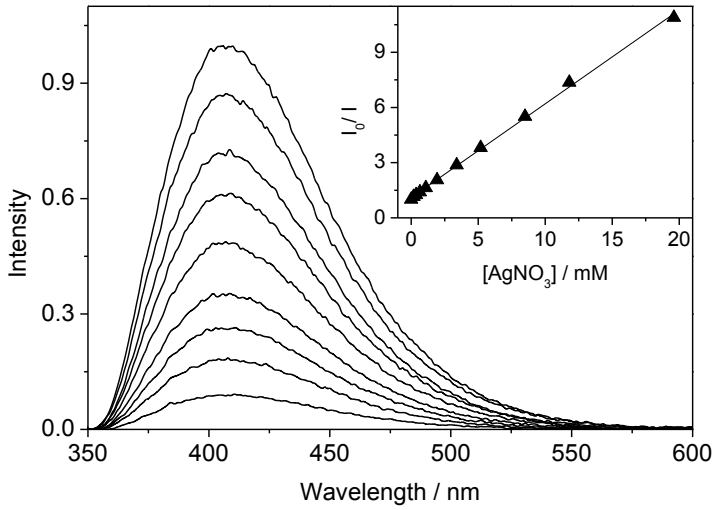

Figure 8. Quenching of the fluorescence of 6.4 μM LuA by 0, 0.18, 0.65, 1.1, 1.9, 3.4, 5.2, 8.5 and 20 mM Ag^{+} in CH_3CN. Inset presents the Stern-Volmer plot of the fluorescence intensity at 410 nm. (λ_{exc}=346 nm)

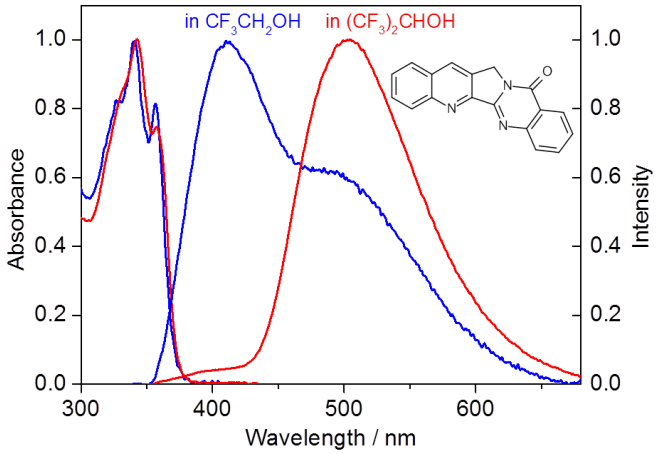

Graphical Abstract

The fluorescence of luotonin A is very sensitive to hydrogen bonding and chelate formation.